Real-Time Multi-Target Tracking with Beamsteering of mmWave Radar Signals

Ubiquitous Computing Term Project Report

by

Sumit Kumar (22CS30056)
Dadi Sasank Kumar (22CS10020)

Under the supervision of

Prof. Sandip Chakraborty

Department of Computer Science and Engineering,

Indian Institute of Technology Kharagpur

November 2025

Abstract

This report details the development of a real-time human detection system using Frequency-Modulated Continuous-Wave (FMCW) mmWave radar. We utilize the Texas Instruments IWR1843BOOST Evaluation Module (EVM) to capture and process radar signals. The core of our system relies on two fundamental principles: the Doppler effect for velocity estimation and Azimuth Analysis (Angle of Arrival) for spatial localization. By implementing a Python-based processing pipeline, we generate and analyze Range-Doppler and Range-Azimuth heatmaps to effectively detect and visualize human motion while distinguishing it from static clutter. This foundational work lays the groundwork for our primary objective: to integrate dynamic beamsteering to enhance signal quality and enable robust multi-target tracking in real-time.

Contents

1 Introduction

Frequency-Modulated Continuous-Wave (FMCW) radar, particularly in the millimetre-wave (mmWave) spectrum, has emerged as a powerful technology for high-resolution sensing. This technology is ideal for detecting and tracking human activity which is being used in this project.

1.1 Motivation: Low Power and Usage Advantages

A primary driver for adopting mmWave radar is its significant advantages over other sensing modalities, especially in ubiquitous and wearable computing.

- **vs. Cameras:** Unlike vision-based systems, mmWave radar is robust to various lighting and environmental conditions (e.g., darkness, fog, or smoke). Furthermore, it preserves user privacy, a critical concern in healthcare and smart home applications.
- **vs. IMUs (Inertial Measurement Units):** Radar offers a fundamentally **contact-free** sensing approach. IMUs must be physically attached to a user, which is often impractical. Moreover, IMUs suffer from **integration drift**, where small, accumulating errors in acceleration lead to significant positional inaccuracy over time. mmWave provides direct, absolute measurements of range and velocity, and thus does not suffer from this drift.
- **Low Power:** For wearable applications like smart glasses, power and form factor are critical constraints. mmWave radar is a low-power solution, with some systems consuming as little as 6 mW [2]. This is a fraction of the power required by camera-based eye-tracking systems, which can exceed 100 mW.
- **Robustness:** The technology is immune to environmental factors that degrade other sensors, such as outdoor sunlight saturating infrared (IR) cameras.

1.2 Advantages of mmWave Radar

The core of a mmWave system relies on fundamental signal processing principles to extract rich information about a target. By analyzing the frequency shift in the reflected wave (the **Doppler effect**), the system can precisely estimate a target's velocity. This is the primary mechanism for detecting motion and, crucially, distinguishing moving targets from static background clutter (e.g., walls, furniture), which will have a velocity of zero.

Furthermore, by using an antenna, the system can perform **Azimuth Analysis (Angle of Arrival)**. By measuring the small phase differences in the signal arriving at different receive (RX) antennas, the system can determine a target's horizontal position. This combination of range, velocity, and angle makes it a far richer sensing modality than single-point sensors like IMUs, which can only measure the motion of the point they are attached to.

1.3 Challenges in Multi-Object Tracking

This standard approach faces significant challenges when applied to multi-target tracking, a primary objective of this project. The literature identifies two critical problems:

- **Insufficient Resolution:** In many real-world scenarios, targets are too close to each other (e.g., two people sharing a bed). The angular resolution of commercial-off-the-shelf (COTS) radars is often insufficient to separate these targets, causing their signals to be merged.
- **Sidelobe Interference:** Even if the radar's resolution is technically sufficient, a problem known as "sidelobe interference" persists. As identified in recent literature, when the radar's main beam is focused on *Target A*, a strong reflection from *Target B* can still leak into the antenna's less-sensitive "sidelobes," creating strong interference that contaminates the signal from *Target A*.

To overcome these limitations, this project will move beyond basic detection. The ultimate goal is to leverage these concepts to implement advanced **beamsteering** techniques, as validated by recent research [3], to dynamically focus the radar's energy. This will enhance the signal-to-noise ratio (SNR) and enable the robust separation and tracking of multiple targets in real-time.

2 Related Work

To guide our project, we reviewed key research papers that demonstrate the advanced capabilities of mmWave radar, from foundational concepts to advanced implementation techniques.

- **Paper 1: *Improving mmWave based Hand Hygiene Monitoring...*** [3]: The work by Nirmal et al. demonstrates the effectiveness of beamsteering for improving micro-gesture recognition at a distance. Their system, BeaMsteerX, steers multiple beams and uses a deep learning model to intelligently combine the data, which significantly enhances the signal-to-noise ratio (SNR) for fine-grained motion.
- **Paper 2: *mmET: mmWave Radar-Based Eye Tracking...*** [2]: Similarly, the research on mmET by Ma et al. highlights the exceptional precision of mmWave radar, showing its capability for sub-millimeter tracking of eye movements. This work utilizes beamforming with learnable weights to improve signal resolution, reinforcing its potential for high-accuracy applications.
- **Paper 3: *Breaking the Resolution Barriers of mmWave Arrays...*** [7]: While the above studies validate beamsteering for enhancing a single target's signal, our project also addresses multi-target tracking. The work by Zhang et al. directly confronts this challenge. They identify that simple beamforming suffers from **sidelobe interference**, where a signal from a second person can contaminate the main signal. They propose **null steering**—placing a direction of zero gain on the interferer—to completely suppress their signal and overcome the resolution limitations of commercial radars in close-proximity scenarios.
- **Paper 4: *Beamforming for Sensing: Hybrid Beamforming...*** [1]: Further exploring advanced beamforming, the "Trebsen" system by Fan et al. introduces a hybrid transmitter-receiver (Tx/Rx) collaboration. Their system can find an optimal **Non-Line-of-Sight (NLoS) path** (e.g., a wall reflection) and use Deep Reinforcement Learning (DRL) to rapidly steer both Tx and Rx beams, ensuring a high-quality sensing path even when the direct line of sight is misaligned.

These studies validate our foundational approach and provide a clear path forward: using beamsteering to enhance detection accuracy and exploring advanced beamforming or null steering techniques as the next step to achieve robust multi-target tracking.

3 Proposed Methodology

Our system is built upon the fundamental signal processing principles of FMCW radar. The methodology involves a processing chain that first estimates the range and velocity of all targets, and then estimates their angle.

3.1 Range Estimation (1D-FFT)

The radar first determines the range to a target by analyzing the "beat signal" (or Intermediate Frequency, IF), which is a mix of the transmitted and received chirps. To resolve multiple targets at different ranges, the system performs a Fast Fourier Transform (FFT) on this signal, known as the **Range-FFT**.

The **Range Resolution**, or the ability to distinguish between two closely spaced objects, is determined by the bandwidth (B) of the signal:

$$\text{Range Resolution} = \frac{c}{2B} \tag{1}$$

Where c is the speed of light. Using our configuration's bandwidth of 3.618 GHz, we achieve a range resolution of 4.14 cm.

3.2 Doppler Effect for Velocity Estimation (2D-FFT)

The Doppler effect is the frequency shift observed from a moving target. To measure this, the radar transmits multiple chirps sequentially in a single "Frame". The phase difference ($\Delta\phi$) between these sequential chirps reveals the target's radial velocity (v):

$$v = \frac{\lambda \Delta\phi}{4\pi T_c} \tag{2}$$

Where λ is the wavelength and T_c is the chirp duration.

- **Working and Approach:** To resolve multiple targets with different velocities, a second **Doppler-FFT** is performed across the chirps for each range bin. This 2D-FFT transforms the data into the **Range-Doppler Matrix (RDM)**, or Range-Doppler heatmap (see Figure 8).
- **Purpose in Human Activity Detection:** This RDM is the primary mechanism for detecting motion. It allows the system to identify moving objects by their non-zero velocity signatures (see Figure 8) and, crucially, to separate them from static clutter (e.g., walls, furniture), which will all appear in the zero-velocity (zero-Doppler) column.

3.3 Azimuth Analysis (Angle of Arrival)

While the RDM tells us *if* something is moving and *how fast*, Azimuth analysis, or Angle of Arrival (AoA), tells us *where* it is in space.

- **Definition:** AoA estimation determines a target's horizontal angular position. The IWR1843 uses a Multiple-Input-Multiple-Output (MIMO) virtual antenna array. As shown in Figure 1, a signal from an angle θ arrives at each receive (RX) antenna at a slightly different time, creating a measurable phase difference across the array.
- **Purpose:** AoA spatially locates targets in the scene. A third FFT is performed across the antenna array data to estimate this phase shift and calculate the angle θ. This is critical for distinguishing between multiple objects that might be at the same range and velocity but at different angular positions. The output is visualized as the **Range-Azimuth heatmap** (see Figure 6).

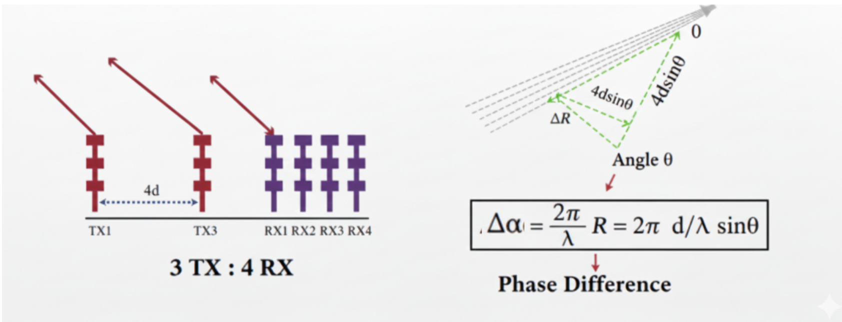

Figure 1: Concept of Time-Division Multiplexing (TDM) MIMO for Angle of Arrival (AoA) estimation, as used in the IWR1843. The angle θ is calculated by measuring the phase shift induced by the extra path length (e.g., $4d \sin\theta$) to different antennas.

3.4 Beamsteering for Enhanced Target Isolation

While the previous techniques provide robust detection and localization, a standard radar illumination has limitations in multi-target scenarios, as discussed in the Introduction. To overcome these, **beamsteering** is employed to dynamically shape the radar's transmitted or received energy.

- **Working Principle:** Beamsteering works by controlling the phase of the signal transmitted from, or received by, individual antennas in an array. By carefully adjusting these phase shifts, the radar can electronically "steer" its main lobe (the direction of maximum energy) towards a specific angle, or create "nulls" (directions of minimal energy) to suppress interference. Figure 2 illustrates how a radar can steer its transmit beams to different angles, focusing energy where it is needed.
- **Purpose in Multi-Target Tracking:** This technique significantly enhances the signal-to-noise ratio (SNR) for a target of interest by concentrating the radar's power in its direction, rather than dispersing it across the entire scene. Conversely, by steering nulls towards interferers, their contaminating signals can be suppressed. This is crucial for separating closely-spaced targets and for robustly tracking multiple objects simultaneously.

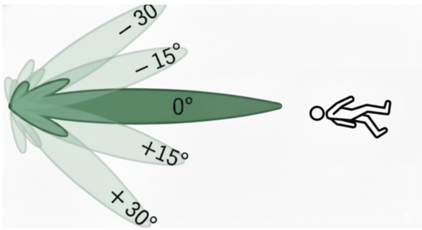

Figure 2: Illustration of dynamic transmit (TX) beam steering. The radar can electronically adjust the phase of signals from its antennas to direct its main beam at various angles (e.g., $\pm 15°, \pm 30°, 0°$), thereby focusing its energy on a target of interest.

4 Implementation

4.1 Experimental Setup

The hardware setup for data acquisition consists of the Texas Instruments IWR1843BOOST Evaluation Module (EVM) and the DCA1000EVM data capture card, as shown in Figure 3. The IWR1843BOOST acts as the primary mmWave sensor, while the DCA1000EVM interfaces with the sensor to capture the raw ADC (Analog-to-Digital Converter) data. This raw data is then streamed to a host PC via an Ethernet connection for real-time processing and visualization.

4.2 Hardware Configuration and Tools

Our initial work involved familiarization with the key hardware and software components. The radar was configured with the parameters specified in Table 1.

- **IWR1843BOOST EVM:** This is the primary sensor platform used for the project. It is a single-chip mmWave sensor operating in the 76-GHz to 81-GHz band, featuring 3 transmit (TX) and 4 receive (RX) antennas, which are essential for Angle of Arrival estimation.
- **TI mmWave Training Series:** We utilized the official training video series [4] to understand the end-to-end signal processing chain, from raw ADC data capture to high-level object detection.
- **OpenRadar GitHub Repository:** We studied the `OpenRadar` repository [5] to understand practical implementations and the structure of the mmWave SDK, which provides the necessary drivers and algorithms for interfacing with the board.

Table 1: IWR1843 Radar Configuration

Parameter	**Value**
Device	TI IWR 1843 3 Tx: 4 Rx: 1
Start Frequency	77Hz
Bandwidth	3.61847 GHz (77 GHz - 80.68 GHz)
Number of Samples	256
Number of Chirps	546
ADC sampling rate	4400 ksps
Frame rate	10 fps
Rx Gain	30
Range Resolution	4.88 cm
Doppler Resolution	0.0806 ms^{-1}

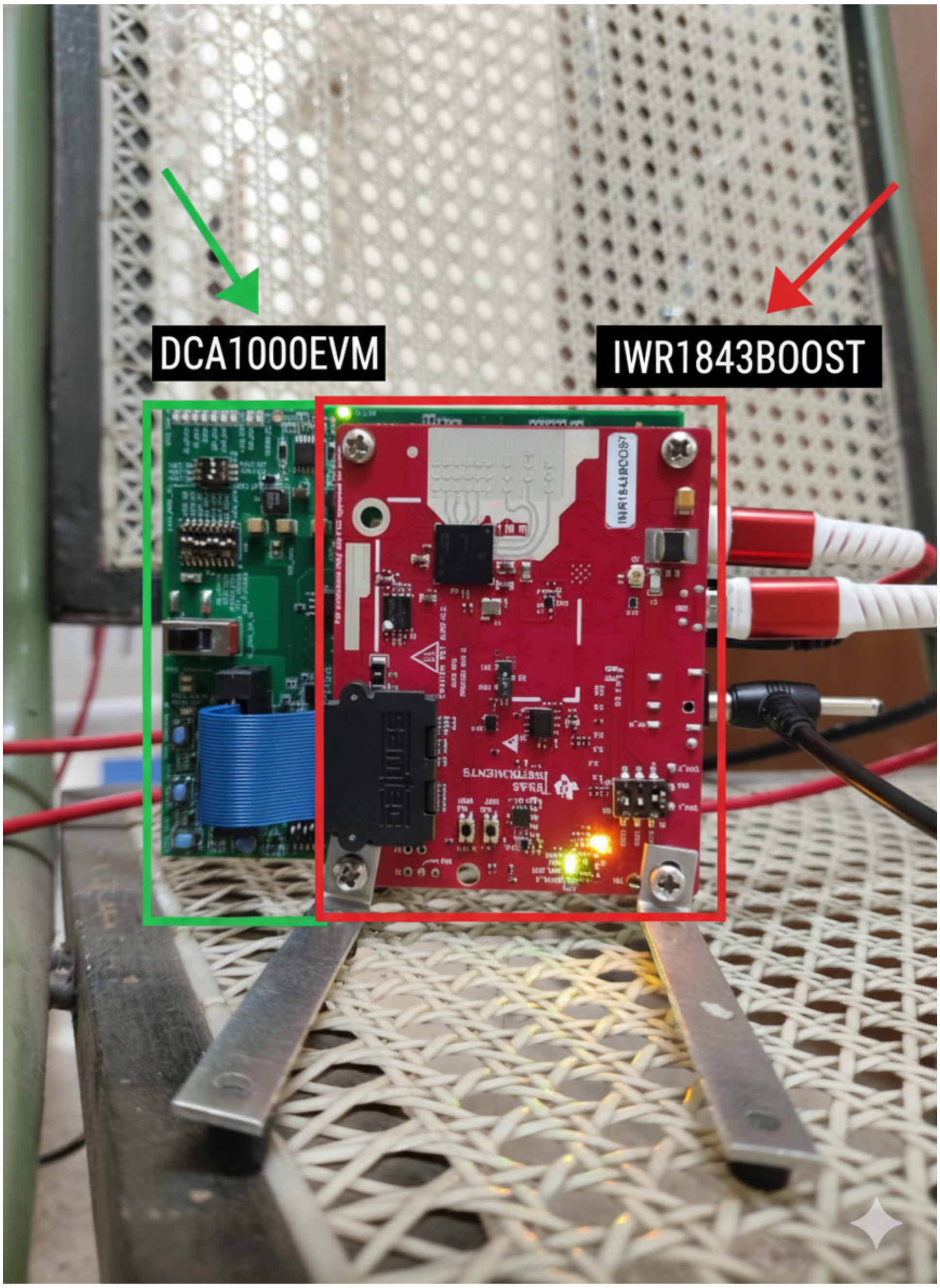

Figure 3: The hardware setup, showing the IWR1843BOOST EVM (left) connected to the DCA1000EVM data capture board (right).

4.3 TX Beamsteering Implementation

A key part of our future work, and a subject of current investigation, is the implementation of transmit (TX) beamsteering. This technique relies on calculating precise phase shifts for each of the radar's transmit antennas to focus the beam at a desired angle (θ).

As derived in the literature [3], the phase shift vector ϕ_N for an antenna array where elements are spaced by multiples of the wavelength (λ) can be calculated. For the IWR1843, the three TX antennas (TX1, TX2, TX3) are spaced at $d_1 = 0$, $d_2 = \lambda$, and $d_3 = 2\lambda$, respectively. This simplifies the phase shift formula to:

$$\phi_N(\theta) = [0, 2\pi \sin\theta, 4\pi \sin\theta] \tag{3}$$

This equation gives the required phase shift in radians for each antenna. These values are then converted to degrees

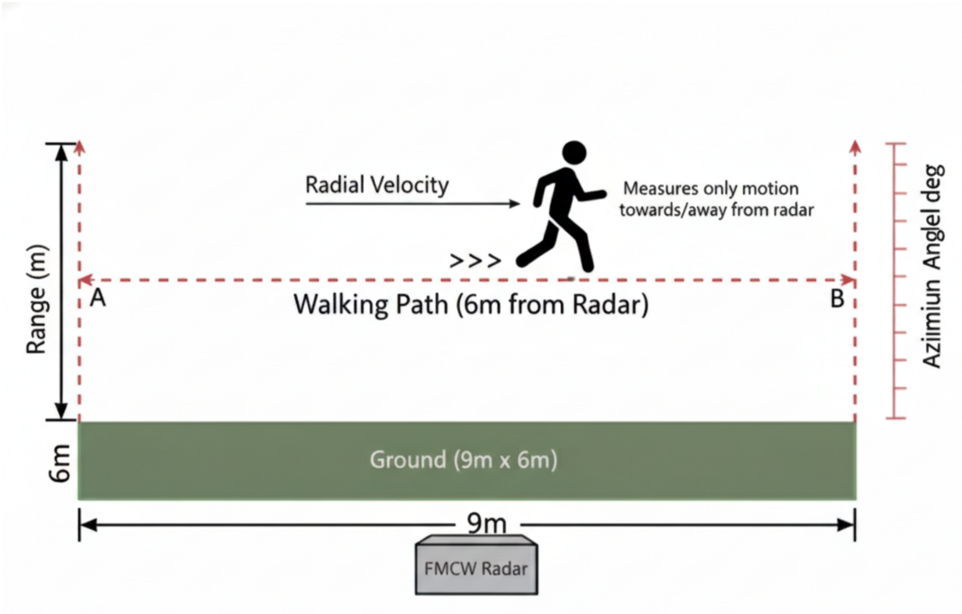

Figure 4: The experimental setup is as shown above, a person moving in front of the radar with dimensions of the ground area.

and programmed into the radar. Table 2 shows the calculated phase shifts required to steer the beam to the angles used in our analysis.

4.4 Formula for Beamforming

The following equation is used in Matlab script was used to calculate the precise phase-shift values (in degrees) required for each of the three transmit (TX) antennas on the IWR1843 board to achieve a desired beam-steering angle (θ). The calculations are based on the antenna spacing of $0, \lambda,$ and 2λ.

$$\phi = \left[\frac{0,\ 2\pi\sin(\theta),\ 4\pi\sin(\theta)}{\pi} \right] \times 180 \tag{4}$$

Table 2: Calculated TX Phase-Shift Values for Beamsteering

Steering Angle (θ)	**TX1 Phase (deg)**	**TX2 Phase (deg)**	**TX3 Phase (deg)**
$+30°$	0.0	15.9889	31.9779
$+15°$	0.0	8.2465	16.5580
$0°$	0.0	0.0	0.0
$-15°$	0.0	-8.2465	-16.5580
$-30°$	0.0	-15.9889	-31.9779

4.5 Beamsteering Validation and Coordinate Transformation

To validate the beamsteering implementation, we collected data at the five specified angles ($0°, \pm15°, \pm30°$). Our initial processing of the point cloud data (PCD) from these captures led to a counter-intuitive finding: all point clouds, regardless of the steering angle, appeared to be oriented in the same direction, as if they were all collected from the $0°$ boresight.

We identified that this was an error in our processing, not in the data collection. The radar's SDK generates point cloud data (x, y, z coordinates) relative to a **local coordinate system** that is *itself* rotated by the steering angle (θ). Therefore, a point detected at $0°$ in the 15-degree-steered-beam's local frame is actually at 15 degrees in the global coordinate system.

To correct this and visualize the true spatial data, we implemented a coordinate transformation, as illustrated in Figure 5. We applied a 2D rotation matrix (around the Z-axis, which is the axis of azimuth rotation) to convert the local coordinates (x_L, y_L) of each point cloud into the global coordinate system (x_G, y_G).

The transformation is given by the equations:

$$x_G = x_L \cos(\theta) - y_L \sin(\theta) \tag{5}$$

$$y_G = x_L \sin(\theta) + y_L \cos(\theta) \tag{6}$$

$$z_G = z_L \tag{7}$$

where θ is the beamsteering angle (e.g., 15°).

After applying this transformation, the results were immediately clear. The point clouds generated from the 15-degree-steered data were distinctly tilted by 15 degrees relative to the 0-degree boresight data. This process validated that our phase-shift calculations and the hardware-level beamsteering were functioning exactly as expected.

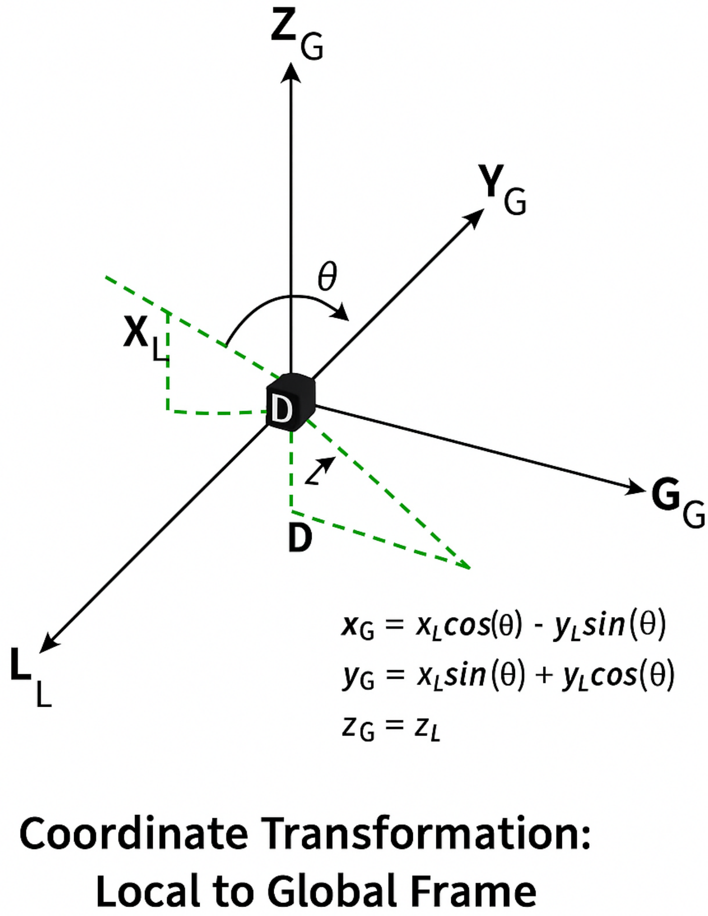

Figure 5: Transformation from the Local Coordinate System (LCS), which is rotated by the steering angle θ, to the Global Coordinate System (GCS). A point $P(x_L, y_L)$ in the local frame must be rotated to find its true position $P(x_G, y_G)$ in the global frame.

4.6 Limitations of Beamsteering Angle

While the phase-shift calculations can be performed for any angle, our validation and the findings in existing paper [3] confirm a limitation. We conducted tests at angles up to $\pm 45°$, but the data from these wider angles was not used in final system.

The reason for this exclusion is not that the data is noisy, but is due to a specific. As explained in [3], the transmit antennas on IWR1843 are spaced by one wavelength (λ) to optimize for TDM-MIMO. A consequence of this design is that when attempting to steer the beam at sharp angles (beyond $\pm 30°$), the **side lobes become more powerful than the main lobe**.

This means that at $\pm 45°$, the radar is sending more energy in undesirable directions (the side lobes) than in the intended direction (the main lobe). This makes the resulting data unreliable for accurate gesture recognition. Therefore, our implementation was restricted to a maximum steering range of $\pm 30°$.

4.7 Processing Pipeline

We developed a Python-based processing pipeline to integrate these concepts and achieve real-time visualization.

- **Data Acquisition:** Raw ADC data is captured from the IWR1843 board via the DCA1000EVM.
- **Range-Doppler Processing:** A 2D-FFT is applied to the raw data. The first FFT (Range-FFT) resolves targets in range. The second FFT (Doppler-FFT) resolves them in velocity.
- **Clutter Rejection:** A simple filter is applied to remove the "zero-Doppler" bin, effectively eliminating static objects from the scene.
- **Peak Detection:** A peak-finding algorithm (such as Constant False Alarm Rate, or CFAR) is applied to the Range-Doppler map to identify potential targets.
- **AoA Estimation:** For each detected peak, a third FFT is performed across the antenna array data to estimate the angle of arrival.
- **Visualization:** The resulting heatmaps and detected target points (with range, velocity, and angle) are plotted in real-time using libraries like Matplotlib or Plotly.

5 Results and Discussions

Our implementation successfully demonstrates the core objectives.

- **Outcome:** We achieved effective detection and animated visualization of human motion.

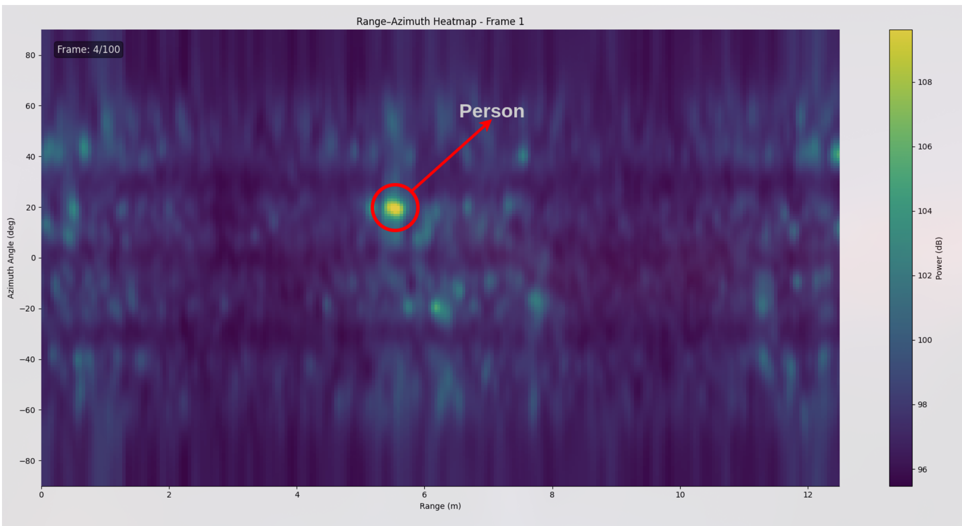

Figure 6: Example Range-Azimuth Heatmap. The peak shows the target at a specific range (Y-axis) and horizontal angle (X-axis).

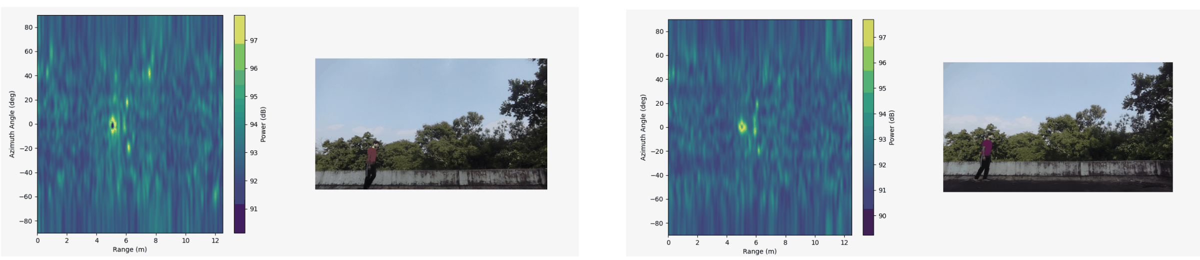

(a) Beam angle: 0°

(b) Beam angle: $+15^\circ$

Figure 7: Range–Azimuth Heatmaps(left-side) aligned with video ground truth(right-side). Each heatmap shows the target peak at the corresponding azimuth angle and range.

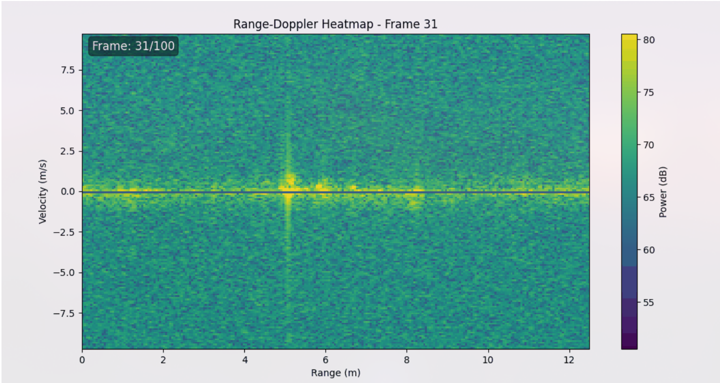

Figure 8: As a person moves sideways relative to the radar, a single peak appears at a particular range. Since there is only slight movement, a strong reflection is observed at that specific range.

6 Conclusion

We have successfully developed a foundational system for real-time object detection and analysis using the IWR1843 mmWave radar. The system effectively implements Doppler processing to detect motion and Azimuth analysis to spatially locate targets, as demonstrated by the real-time generation of Range-Doppler and Range-Azimuth heatmaps.

7 Future Work

The current system provides a illumination, which is not optimized for tracking multiple, closely-spaced targets.

Our future work will focus on three key areas:

1. **Real-Time Dynamic Beam Steering:** We plan to transition from static beam testing to a dynamically that adjusts the phase shifts of the transmitter (TX) antennas. This will allow the radar to electronically steer the main lobe toward regions of interest in real-time, significantly enhancing the Signal-to-Noise Ratio (SNR) by focusing energy where it is needed most.
2. **Multi-Target Tracking using Kalman Filter:** To maintain persistent tracks for multiple simultaneous targets, we will implement a state-estimation algorithm, such as a Kalman filter. This framework will correlate detections across sequential frames, smoothing out trajectory noise and establishing a robust motion history for each distinct object in the scene.
3. **Enhanced SNR and Cluster-based Centroid Tracking:** Using the Point Cloud Data (PCD) resulting from SNR, we will refine our pipeline. We will use density-based clustering (DBSCAN) to group target reflections and compute intensity-weighted centroids. These precise coordinates will serve as stable measurement inputs for the tracking system, reducing and improving spatial accuracy.

References

[1] Long Fan, Lei Xie, Wenhui Zhou, Chuyu Wang, Yanling Bu, and Sanglu Lu. 2024. Beamforming for Sensing: Hybrid Beamforming based on Transmitter-Receiver Collaboration for Millimeter-Wave Sensing. *Proc. ACM Interact. Mob. Wearable Ubiquitous Technol.* 8, 2, Article 75 (June 2024). https://doi.org/10.1145/3659619

[2] Ruichun Ma, Yasuo Morimoto, John S. Ho, Sam Shiu, and Jiang Zhu. 2025. mmET: mmWave Radar-Based Eye Tracking on Smart Glasses. *The 23rd ACM Conference on Embedded Networked Sensor Systems (SenSys '25)* (May 2025). https://doi.org/10.1145/3715014.3722050

[3] Isura Nirmal, Wen Hu, Mahbub Hassan, Elias Aboutanios, and Abdelwahed Khamis. 2025. Improving mmWave based Hand Hygiene Monitoring through Beam Steering and Combining Techniques. *The 23rd ACM Conference on Embedded Networked Sensor Systems (SenSys '25)* (May 2025). https://doi.org/10.1145/3715014.3722085

[4] Texas Instruments. 2025. mmWave Training Series. https://www.ti.com/video/series/mmwave-training-series.html. Accessed: October 2025.

[5] The OpenRadar Initiative. 2025. OpenRadar GitHub Repository. https://github.com/presenseradar/openradar. Accessed: October 2025.

[6] The Work Codefiles. [n. d.]. Implementation GitHub Repository. https://github.com/SumitKumar-17/OpenRadar. Accessed: October 2025.

[7] Duo Zhang, Xusheng Zhang, Zhehui Yin, Pengfei Zhou, Hongliu Yang, Pei Wang, Zhiyun Yao, Junzhe Wang, Fusang Zhang, and Daqing Zhang. 2025. Breaking the Resolution Barriers of mmWave Arrays via Null Steering for Sleep Monitoring in Multi-Person Scenarios. *Proc. ACM Interact. Mob. Wearable Ubiquitous Technol.* 9, 3, Article 149 (September 2025). https://doi.org/10.1145/3749466